Part 3

NANOCOMPOSITES AND SEMICONDUCTOR NANOSTRUCTURES

18 Micro-domain Engineering for Optics and Acoustics

Shi-ning Zhu, Yong-yuan Zhu and Nai-ben Ming
National Laboratory of Solid State Microstructures, Nanjing University, Nanjing 210093, China

1 INTRODUCTION

For the recent two decades, inspired by the success of the semiconductor superlattice and quasi-phase-matching (QPM) technique, ferroelectric superlattice has become a hot topic in material science and photoelectronics. One expects that the material can provide new means to control and manipulate light and ultrasonic by means of its unique functions.

Ferroelectric superlattices may consist of two kinds of ferroelectric materials or of ferroelectric and non-ferroelectric materials layer by layer alternatively, forming so-called heterostructures. However, most of them consist of the same kind of material, such as single crystals, in which the modulated structure is ferroelectric domain. All physical properties associated with third-rank tensor in such a superlattice will be modulated with domain, whereas those associated with even-rank tensor remain constants. It is the modulated physical properties that make the material different from the homogeneous single domain crystal, and specially favorable for applications in nonlinear optics and ultrasonic. In particular, when the wavelength of optical or ultrasonic wave is comparable with or smaller than the size of domain, that is, the reciprocal vectors of the modulated structure are comparable or larger than the wave vectors of optical and ultrasonic waves. Many fancy physical effects may generate through the interaction of the wave vectors and the reciprocal of superlattice. For example, the enhancement of quasi-phase-matched optical frequency conversion, the generation of squeezed light, the electro-optic deflection and the excitation of high-frequency ultrasonic *etc.* The interests in ferroelectric superlattice lie not only in its fundamental research but also in practical applications. Many of them have been put to use in novel optical and acoustic devices matched with contemporary photoelectric technology.

2 MODULATED DOMAIN STRUCTURES

Although there may be various kinds of domain orientations in different ferroelectric crystals, most of current ferroelectric superlattices are mainly composed of 180° anti-parallel laminar ferroelectric domains. One can formally construct a ferroelectric superlattice as follows: defines one or a couple of basic blocks first, and each consists of a pair of anti-parallel laminar domains, one positive and the other negative, then arranges it for them according to some production rules or sequences.

Periodic superlattice is the simplest one that has just one basic block arranged with a simple repetition, while quasi-periodic superlattice is composed of two basic blocks or more. The neighbouring domains in such a structure are interrelated by a dyad axis due to the fact that their orientations of spontaneous polarizations P_s are of opposite sign as illustrated in Figure 1(a). There are two kinds of 180° domain configurations: one is P_s parallels to the domain wall with an "anti-parallel" configuration as shown in Figure 1(b) and the other is P_s perpendiculars to the domain wall with a "head-to-head" configuration as shown in Figure 1(c). Due to no freedom surface in the second case, the bound charge on the boundary is not being screened effectively, therefore, the boundaries of adjacent domains are charged with opposite sign. The arrows in Figures 1(b) and (c) indicate the directions of the P_s in these two configurations, respectively. All physical properties with odd-rank tensor, such as second-order nonlinear optical coefficient d_{ijk}, electro-optic coefficient γ_{ijk} and piezoelectric coefficient h_{ijk}, are no longer constants in the crystal, instead, change their signs from positive domain to negative domain, and become a function of the spatial coordinates (Figure 1(d)). Therefore a factor $f(x)$ should be included in them where

$$f(x) = \begin{cases} +1 & if \quad x \quad is \quad in \quad the \quad positive \quad domains \\ -1 & if \quad x \quad is \quad in \quad the \quad negative \quad domains \end{cases}. \tag{1}$$

The f (x) may be a periodic, quasi-periodic or aperiodic function, depending on the sequence of ferroelectric domain in a superlattice. Figure 1(e) is an optical micrograph of $LiNbO_3$ (LN) with periodically modulated domains.

3 FABRICATION METHODS

As mentioned above, most of ferroelectric superlattice is composed of 180° anti-parallel laminar domains. A variety of techniques for controlling domain patterns in ferroelectric crystals, either during or after growth, have been developed. Among them, growth striation technique (Ming *et al.*, 1982), field poling technique (Yamada *et al.*, 1993), electron writing (Ito *et al.*, 1991) and Corona poling are mainly used for bulk ferroelectric crystals, while chemical diffusion and substitution of impurities for waveguide materials (Webjorn *et al.*, 1989). In spite of making progresses, many of these techniques remain semi- empirical in which the mechanisms of polarization reversal are poorly understood. Nevertheless, this does not prevent them as practical methods to fabricate the various ferroelectric superlattices for different applications.

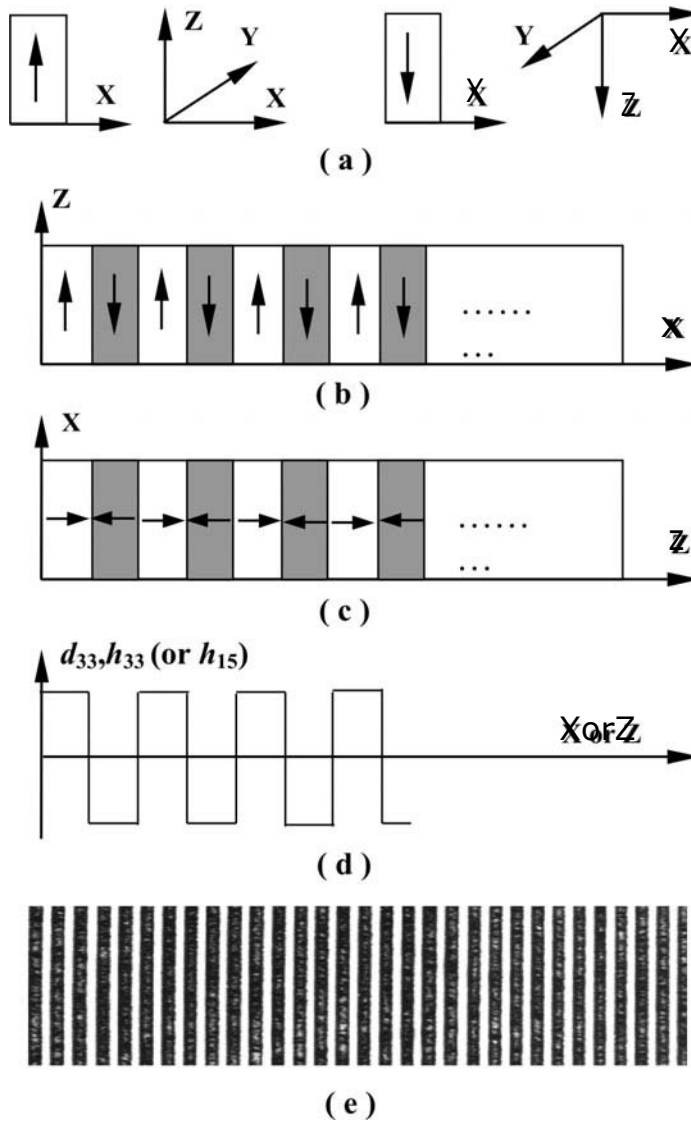

Figure 1: (a) Positive domain (↑), negative domain (↓) and their coordinate systems.
(b) Periodic superlattice with the spontaneous polarization modulated along the x-axis.
(c) Periodic superlattice with the spontaneous polarization modulated along the z-axis.
(d) Corresponding second-nonlinear optical coefficient, piezoelectric coefficient as a periodic function of x (z).
(e) An optical micrograph of $LiNbO_3$ superlattice with periodic laminar ferroelectric domains, corresponding to the arrangement (b) and (c).

3.1 Growth Striation Technique

Fabrication of ferroelectric superlattice using growth striation technique was first accomplished by Feng and Ming *et al.* (1980) in a Czochralski system. The technique has been successfully used to grow LN (Lu *et al.*, 1996), $LiTaO_3$ (LT) (Wang *et al.*, 1986), and $Ba_2NaNb_5O_{15}$ (BNN) (Xu *et al.*, 1992) superlattices. Feisst and Koidl (1985), and some other groups respectively reported their works on fabricating LN superlattices using similar growth methods.

In the method the melt is doped with solute to control domain structure, such as yttrium, indium or chromium for LN, with concentration about 0.1 wt.% - 0.5 wt.%. Ming *et al.* (1982) found that a temperature fluctuation may be introduced into the solid-liquid interface, either through an off-axis rotation or through applying an alternating electric current. The temperature fluctuation causes a spatial modulation of the impurity or composition in crystal along the growth direction. The effect can form a space charge distribution, and in turn induce a local electric field in crystal. When cooling through the Curie point, the field plays a key role of causing *in-situ* and local laminar domain. The modulated domain structure may automatically realize during the cooling process of crystal. Obviously the domain structures and the solute distribution should have the equal period. The period or structure parameter of domain may be adjusted by choosing suitable pulling rate and rotation frequency or by changing the period of modulating electric current.

Figure 2 shows the measured temperature fluctuations at solid-liquid interface (Figure 2(a)) and the formed growth striations (Figures 2(b)) for LN crystal. Ming *et al.* demonstrated the one-to-one correspondence between the growth striations and the laminar domain structure (Figures 2(c) and (d)). The relationship between solute fluctuation and the ferroelectric domain structure has also been revealed with x-ray energy dispersive spectrum analysis. Figure 3 is the measured result of a LN crystal sample doped with yttrium. This figure shows domain walls are always situated at the places where the gradient of the Y solute concentrations changes its sign from plus to minus or vice versa.

A significant progress was made by Magel *et al.* (1990), who used laser-heated pedestal growth to prepare a LN single crystal fibre. Domain pattern with 2-3.5 μm period in the fibre of ~250 μm diameter was achieved by periodically modulating the heating power. The mechanism in the method is similar to that in growth striation technique. Jundt *et al.* (1991) used the single crystal fibre with 1.24 mm long and a 3.47 μm domain period for a second harmonic green generation of 2 W from a 4 W, 1.064 μm fundamental source. It is the first report for LN superlattice to be operated at average power at Watt level.

An advantage of the growth striation technique is that the sample prepared has a large cross section, which can avoid tight position alignment tolerance and results in a higher output in optical applications. Another advantage of the method is that it is easy to dope some laser active ions into the crystal during growth for

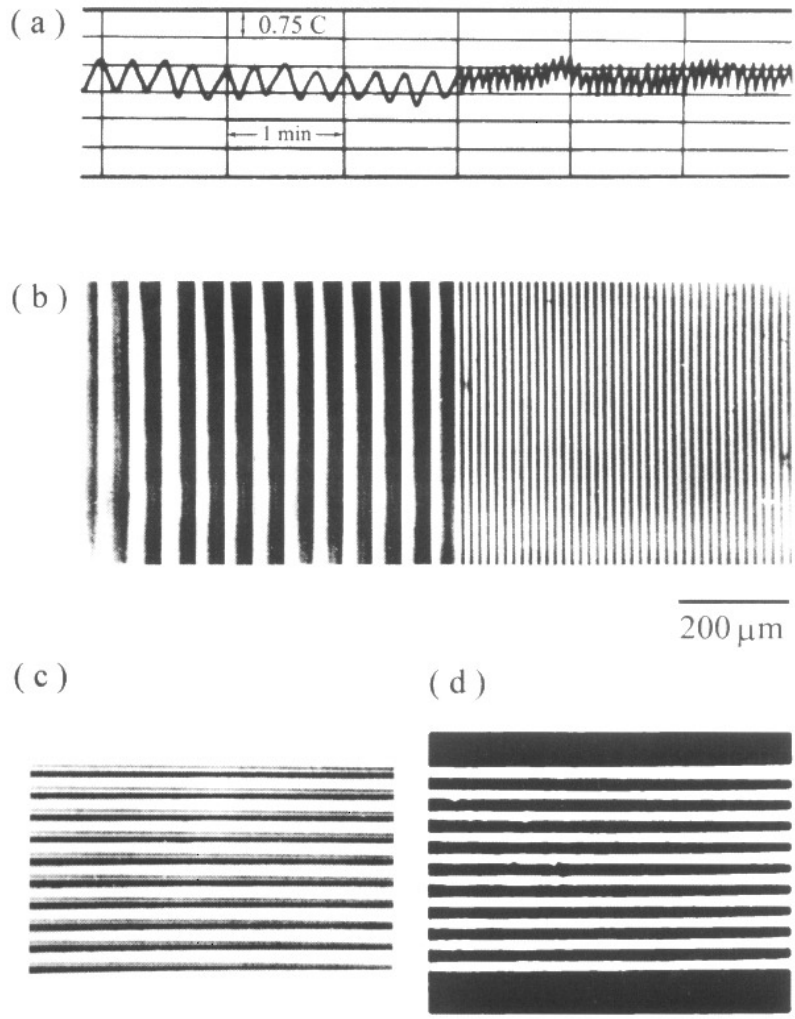

Figure 2: Temperature fluctuations measured on the solid-liquid interface (a) and the corresponding surface rotational growth striations in a LN crystal (b), while rotational rate was changed suddenly from 4 to 13 rpm in the experiment. Surface rotational growth striations (c) and the corresponding interior laminar ferroelectric domain structures (d). [after Ming *et al.*, 1982]

the design of multifunction laser device. Lu *et al.* (1996) and Zheng *et al.* (1998) doped Nd^{3+} and Er^{3+} ions into the LN superlattice crystals, respectively. The nonlinear optical properties of substrate crystal and spectral properties of Nd^{3+} or Er^{3+} ions were combined in the same superlattice. The spectral structure (including

absorption and fluorescence spectra) of these superlattices is generally similar to those of doped crystals with single domain or glass fibres, verifying no obvious effect of domain wall for the excitation properties of doping ions.

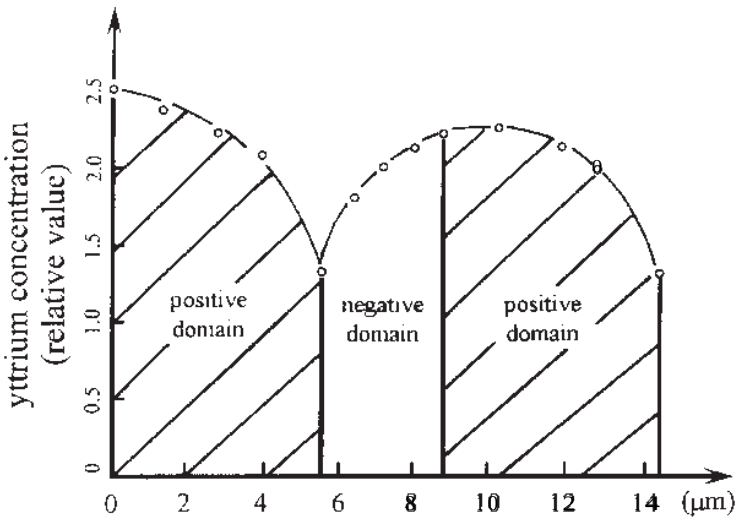

Figure 3: The yttrium concentration distribution and ferroelectric domain structures in rotational striations. The yttrium concentration measured using X-ray energy dispersive spectrum analysis, point by point, along the modulation direction of domain. It is worth noting the domain boundaries are situated at places where the gradient of yttrium concentration changes its sign. [after Ming *et al.*, 1982]

3.2 Chemical Diffusion

In 1979, Miyazawa (1979) discovered that the diffusion of element titanium (Ti) could give rise to the domain reversal on the + z surface of LN crystal. Later, it was confirmed that proton or ion exchange followed by heat treatment could also produce domain reversal on the + z face of LN (Zhu *et al.*, 1995), and the – z faces of LT (Ahlfeldt, 1994) and $KTiOPO_4$ (KTP) (Vanherzeel and Bierlein, 1992), respectively. Following these discoveries, the chemical diffusion and impurity ion exchange were exploited to fabricate the periodically domain reversal patterns located within a few microns of the surfaces of the LN, LT and KTP crystals. These two methods were appropriate for guided wave interactions and surface acoustic wave devices. Their advantage is that the metal mask, defined by lithography, is deposited on the surfaces prior to Ti diffusion or proton exchange, which can lead to a well-defined domain period when domain reversal occurs. The

disadvantage is that the shape of the reversed domain is either triangular (for Ti diffusion in LN) or semi-circular (for proton exchange in LT). The shapes of reversed domains are not ideal for optical or acoustic applications. However high conversion efficiencies were still obtained in waveguide devices due to long effective interaction length and tight confinement of beam in the geometry (Yamada *et al.*, 1993).

A possible explanation to the domain reversal mechanism of Ti diffusion was given by Peuzin (1986) according to the earlier works of Thaniyavarn *et al.* (1985), Tasson *et al.* (1976) and Ming *et al.* (1982). Ming and Tasson had certified that an impurity concentration gradient in LN had the same poling property as an electric field (equivalent field). This mechanism might apply more generally for the chemical diffusion and heat treatment methods.

3.3 Electron Beam Writing

Electron beam has been used to induce a modulated domain structure in some ferroelectric crystals by writing on the negative polarity surfaces of these crystals directly. Keys *et al.* (1990) and Ito *et al.* (1991) first made progress in LN, whereafter, Hsu *et al.* (1992) in LT and Gupta *et al.* (1993) in KTP, respectively, using a scanning electron microscope (SEM). In a typical experimental geometry, the + c surface of the crystal was coated with 50–150 nm Au, Al, Cr or other metal film, and mounted on the SEM sample stage. The electron beam is focused and scanned on the uncoated – z face of the crystal. The acceleration voltage of the electron beam is sample dependent. It is 20–25 kV for a LN wafer with 0.5 mm thickness. The beam current and beam size fallen on the surface of sample ranges within several *p*A–several *n*A and from 0.3–0.5 μm, respectively, depending on the period of domain and scanning speed that is generally set from 0.02 mm/s to 0.1 mm/s. The penetration depth of the electron into treated sample depends on the electron energy and the nature of material. It is estimated to be about a few micrometers for most ferroelectric crystals. The domain reversal can steadily extend across the sample wafer, under certain conditions, and the thickness can reach to 1 mm for LN crystal, which is several hundred times greater than the electron penetration depth. This method provides a domain wall perpendicular to the surface. The mechanism for the domain reversal by the electron beam is not very clear at this moment, however, a volume domain grating can be fabricated in the ferroelectric sample. LN, LT and KTP superlattice with period 3–7 μm were fabricated by the method and a high efficient second harmonic green and blue light were generated by the bulk and waveguide experimental geometry, respectively. Mizuuchi *et al.* (1994) reported that ion-beam writing induced the domain reversal in a LN or LT crystal wafer, therefore can also be used to fabricate ferroelectric superlattices.

3.4 Electric Field Poling

Although electron and ion writing can be used in the fabrication of small periodic domain gratings, it is in practice limited by the slow writing speed and the complicated and expensive beam scan system. A definite goal for practical applications is to find a technique that can mass-produce modulated domain materials at low cost. Yamada and his co-worker (1993) realized a significant breakthrough along this direction in 1992. They successfully fabricated a periodic domain grating in a ~ 0.2 mm thick LN thin wafer by applying a pulsed field at room temperature. The periodicity of the domain structure was defined by the lithographically fabricated metal electrode. They also confirmed that the periodic electrode should be fabricated on the positive z face of LN for the reversed domain nucleates more easily on the + z face than on the – z face. By using this technique, great progress has been made towards fabricating thicker samples as well as other ferroelectrics, such as LT, KTP, SBN *etc.*

The details for field poling on LN, LT, KTP and SBN crystals at room temperature were described by Miller (1998), Zhu *et al.* (1995), Rick and Lau (1996) and Zhu *et al.* (1998). In this method, the location of the reversed domains is defined by the lithographically fabricated electrode and the domain duty cycle is controlled by the spacing ratio of electrode and switch time t_s. The t_s should be selected according to the expression $Q = \int_0^{t_s} i dt = kP_S A$, where Q is the total delivered charge, k a coefficient around 2.2 – 2.5 from experiential, and P_s and A are the spontaneous polarization and total area of reversed domain, respectively. For a periodic structure, the area $A = N \cdot d \cdot l$, here N is the period number of superlattice, d is the average width of the reversed domains, and l is the average length of reversed domains. If the period of a superlattice is Λ, the duty cycle $\rho = d/\Lambda$. Miller (1998) proposed that domain reversal under periodic electrodes could be divided into several stages. First, domain nucleates along each strip electrode edges. Then, domain apex propagates toward the opposite face. Once the apex reaches the – z face, it extends rapidly and coalesces under the electrode and extends out of the area covered by electrode strips. The duty cycle of the domain is controlled by the electrode width, and amplitude and duration of the applied field. For small-period patterns (Λ<10 μm), the width of the electrode is generally designed not to exceed $\Lambda/4$ to avoid domain merging prior to coalescence and the field amplitude is set at the field with the value of highest nucleation site density. In conventional poling, in order to prevent the back-switching effect (Fatuzzo and Merz, 1967), the external field is ramped to zero over a duration of ~ several tens ms to stabilize the reversed domains, instead of removing it abruptly.

By far, most of the LN and LT superlattices are made of congruent composition crystals, because they are easy to grow and are available commercially with high quality and low price. Recent progress in growth technique makes it possible to grow LN and LT with stoichiometric. Gopalan *et al.* (1998) and Kitamura *et al.* (1998) found that the electric field for domain reversal in the stoichiometric crystals was much lower than in congruent crystals, and the values are about one-fifth for LN and one-thirteenth for LT, respectively. However,

the spontaneous polarizations P_s and the Curie temperature were relatively insensitive to the nonstoichiometry. The internal fields in congruent crystals, which were calculated from the asymmetry in the P_s versus electric field hysteresis, disappeared in stoichiometric crystals. These results further verify that the origin of the internal field and large changes in the poling fields of LN and LT appear to be largely dependent on the ratios of [Li]/[Li + Nb] and [Li]/[Li + Ta], therefore, on nonstoichiometric point defects in these two crystals, respectively. There are interests aroused about the stoichiometric crystals because lower poling field and better poling characteristic make them candidates for poling thicker samples (thicker than a few millimeters) to fabricate bulk devices for nonlinear optical application.

Recently, Batchko *et al.* (1999) further improved electric field poling technique that incorporates domain back-switching as a means for realizing high-fidelity short-period domain pattern essential for SHG of blue and UV light. High-quality LT superlattice with period as short as 1.7 μm was prepared for UV second-harmonic-generation (SHG) (Mizuuchi *et al.*, 1997). LN (Burr *et al.*, 1997), SBN (Zhu *et al.*, 1997e) and KTP (Wang *et al.*, 1998) superlattices with 1 mm thickness were fabricated successfully.

The superlattices with various domain gratings, such as chirped period (Loza-Alvarez *et al.*, 1999), quasi-period (Zhu *et al.*, 1997, 1998), Thue-Morse structure and domain lens and prism array (Yamada *et al.*, 1996, Chiu *et al.*, 1996) were fabricated had used the above method as well. The poling properties of various doped LN, LT, SBN and KTP crystals have also been studied at room temperature and at low temperatures (~170 K) (Rosenman *et al.*, 1998). These studies enables significant optimization of the process parameters. It was reported that the electric field poling had been accomplished in LN wafers up to 3 inch in diameter, 5 cm in device length and 0.5 mm in thickness (Byer, 1997).

4 LINEAR AND NONLINEAR OPTICAL EFFECTS

Wave vector conservation plays an important role in interactions between electromagnetic waves and media, no matter whether the interactions are linear or nonlinear. One widely known example is the Bragg condition in X-ray diffraction, where the wave vector conservation between the incident and diffracted waves is fulfilled with a reciprocal vector provided by the crystal lattice. In optical materials, such as photonic crystals, the refractive index modulation leads to Bragg reflection and formation of band gaps, so that light waves with frequency within the gap is forbidden to propagate. The treatment can be extended to a ferroelectric superlattice in which the electro-optic effect can introduce the modulation of refractive index. Although the refractive index modulation originated electro-optic effect is not strong enough, it is adjustable by extend field. In the nonlinear optical regime, most phenomena are related to parametric interactions and the Kerr-effect. The wave vector conservation in parametric interactions, such as SHG and third-harmonic-generation (THG) *etc.*, is just the so-called phase matching condition. The second-order nonlinear coefficient $d(x)$ in a ferroelectric

superlattice is modulated by domain. As a result, in the superlattice, the generated parametric wave has a π phase shift when passing through the domain boundary. The phase shift will offset the phase difference between the generated wave with the exciting wave due to the dispersion of refractive index, thus a quasi-phase-matching is fulfilled.

4.1 Electro-optic Effects

In the linear optics regime, physics effects in a ferroelectric superlattice mainly involved in modulated electro-optic coefficient r_{ijk}. As a third-rank tensor, its elements have opposite signs in a positive and a negative domain. In the presence of an external field along some axis of the crystal, the modulation of electro-optic

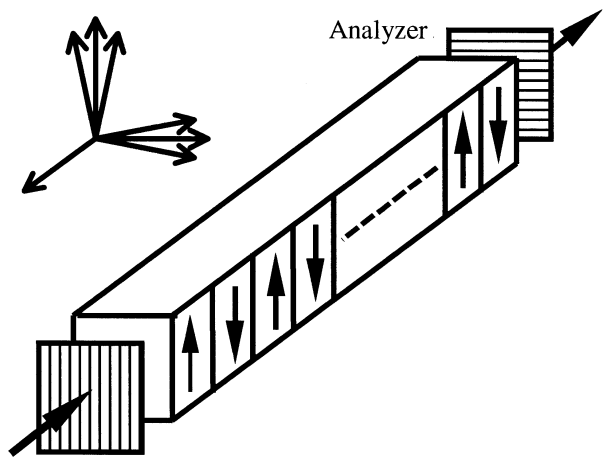

Figure 4: Schematic diagram of an OSL electro-optic system. *X, Y, Z* denote the principal axes of the unperturbed dielectric tensor, and X_N, Y_N, Z_N and X_P, Y_P, Z_P are the principal axes of the perturbed dielectric tensor of negative and positive domains, respectively.

coefficient will accordingly lead to the modulation of refractive index, or the alternating rotation of the principle axis due to the deformation of the refractive index ellipsoid in the superlattice. Lu *et al.* (2000) and Zhu *et al.* (1992) studied electro-optic effects and transmission spectra in a periodic and a quasi-periodic LN superlattice, respectively. Figure 4 is a schematic diagram that shows the electro-optic effect in a LN superlattice. The electrodes are coated on the *y* surfaces of the superlattice. In the absence of an external electric field, the principle axes of the positive domains overlap with those of the negative domains

and the dielectric tensor has only diagonal components with respect to the principle axes. The superlattice is homogeneous to the propagation of light in the linear optics regime. There is no refractive index modulation accompanying the domain modulation. In the presence of an external electric field, however, dielectric tensor is perturbed because of the electro-optic effect, which results in a small dielectric modulation along the propagation direction of light. The new dielectric principle axes may no longer overlap due to the cause that new off-diagonal components appear in their original dielectric tensors. The new principle axes rotate from the original principle axes by an angle with opposite signs in positive and negative domains, respectively. The angles depend on the applied external field. In Figure 4, the initial condition at $x = 0$ which is determined by the polarizer is given by $E_y(0) = 0$ and $E_z(0) = 1$, where E_y and E_z are the mode amplitudes for y - polarized and z - polarized light, respectively. According to the coupled-mode theory (Yariv and Yeh, 1984), Lu *et al.* (2000) and Zhu *et al.* (1992) considered the coupling effect of light beams with orthogonal polarization in a periodic and a quasi-periodic superlattice, respectively. They found that the energy could be transferred back and forth between these two orthogonal modes in this electro-optic system. At the analyzer (y-polarized), i.e. $x = L$ (which is directly related to the number of domain blocks), E_z is extinguished, and the transmission of the y-component is wavelength dependent and is controllable by an applied electric field. Their results verify that the periodic and quasi-periodic superlattices are similar to adjustable Solc filters. Moreover, Lu *et al.* (1999) proposed an electro-optic tuning scheme to tune the output frequency of a quasi-phase-matched optical parametric oscillator (OPO). Compared to temperature tuning, electro-optic tuning provides a faster time response. The tuning rate was expected to excess 3 nm/(kV/mm). Recently Lu *et al.* (2000) proposed a high-frequency travelling-wave integrated electro-optic modulator based on a periodically poled LN. The travelling velocity of the optical wave and the electrical wave velocity in the waveguide can be quasi-matched due to the periodic structure. Using this design, a wide-bandwidth electro-optic modulator with several hundred GHz can be realized.

The modulated anti-parallel ferroelectric domains with different geometric patterns have been used to focus, switch, and deflect a light beam through electro-optic effect. Yamada *et al.* (1996) and Chiu *et al.* (1996) prepared the electric-field induced cylindrical lens, switching and deflection devices composed of the inverted domain array. These micro-optical devices can align the light beam and yield high-quality optical systems at low cost, therefore, they are especially suitable for integrated optics fabricated in ferroelectric substrates.

4.2 Quasi-Phase-Matched Frequency Conversions

Efficient second order nonlinear interactions, such as SHG and other optical parametric process, require a tool to achieve phase matching of the interacting waves over the interaction distance of these parametric waves. The process is

easier understood in wave vector space. The reciprocal vector, originating from the modulation of nonlinear coefficient $d(x)$ in a superlattice, may compensate for the wave vector mismatching of parametric waves, making this process quasi-phase-matched. According to Fourier transform, the $d(x)$ of a periodic superlattice can be written as

$$d(x) = \sum_m d_m \exp(iG_m x), \tag{2}$$

where the reciprocal, $G_m = 2m\pi/\Lambda$, m is an integer and Λ is the period. For a SHG process, QPM condition, or wave vector conservation, is written as

$$\Delta k = k_2 - 2k_1 - G_m = 0, \tag{3}$$

where k_2 and k_1 are the wave vectors of harmonic and fundamental wave, respectively, and m presents the order of QPM. Under QPM condition, the fundamental wave can be effectively transferred to harmonic wave. The efficiency of SHG, in the small signal approximation, is given as

$$\eta_{2\omega} \propto (d_m L)^2 I_\omega \, sinc^2(\Delta k\, L/2). \tag{4}$$

When $\Delta k = 0$, the *sinc* function equals one, hence the second harmonic signal grows quadratically with crystal length L and effective nonlinear coefficient d_m. In practice, only a few G_m with lower indices, such as G_1, G_2 and G_3, can produce significant efficiency in frequency conversion for they correspond to larger Fourier component than those with higher indices (Fejer *et al.*, 1992).

The advantage of QPM is that it permits access to the highest effective nonlinear coefficient of the material, that is, the diagonal component of the d_{ijk} tensor, thus providing higher conversion efficiency. In lithium niobate, QPM with all waves polarized parallel to the z axis yields a gain enhancement over the birefringence phase matching of $(2d_{33}/d_{31})^2 \approx 20$. Another advantage of QPM is that any parametric interaction within the transparency range of a nonlinear material can be noncritically phase matched at any required temperature, even interactions for which birefringence phase matching is impossible (for example, in GaAs, ZnSe and LT crystals *etc.*)

QPM condition in other parametric processes can be written into an expression similar to Equation (2). For example, for a sum-frequency generation in a periodic superlattice, it reads

$$\Delta k = k_3 - k_2 - k_1 - G_m = 0, \tag{5}$$

where $\omega_3 = \omega_2 + \omega_1$, k_3, k_2, k_1 are the wave vectors of ω_3, ω_2, ω_1, respectively, and G_m is the reciprocal vector of the superlattice that satisfies $\Delta k = 0$. When $\omega_2 = \omega_1$, $\omega_3 = 2\omega_1$, Equation (5) degenerates into Equation (3).

As early as in 1980, Feng and Ming (Feng *et al.*, 1980) first prepared a LN superlattice using growth striation method. With this crystal, the QPM theory was experimentally verified. Feisst and Koidl (1985) performed an experiment with a

LN superlattice prepared through the application of an alternating electric current during the growth process. Magel *et al.* (1990) realized the QPM blue light SHG in a LN fiber. In 1990s, the QPM technique, spurred by the need for blue light laser sources for data storage, compact disc players and laser display etc., has made great progress. High efficiency QPM second harmonic generation has been demonstrated in bulk LN and KTP superlattices in both *cw* and pulsed regimes (Robert *et al.*, 1999). For example, single-pass *cw* and quasi-*cw* SHG with efficiencies as high as 42% (Miller, 1998) and 65% (Pruneri *et al.*, 1996) were realized in LN superlattice, respectively. Internal conversion efficiency of 64% was achieved using a KTP superlattice for single-pass SHG of high-repetition-rate, low-energy, diode-pumped lasers (Englander *et al.*, 1997). By placing a KTP superlattice in an external resonant cavity, conversion efficiency of 55% was obtained for a *cw* Nd:YAG laser (Arie *et al.*, 1998). When used for OPO, ferroelectric superlattices show advantages such as high gain, low threshold and engineerability of domain structures, which make it possible to develop a robust, all solid-state, diode-pumped, miniaturized OPO (Burr *et al.*, 1997). Diode laser-pumped solid-state lasers, in particular the Nd laser, in which diode lasers replace flashlamps, have been used as pump sources for OPOs, resulting in compact sources of widely tunable coherent radiation (Cui *et al.*, 1997). Recently, Ferroelectric superlattices, including both LN (McGowan *et al.*, 1998) and RTP, have extended tuning further into the mid-infrared (6.5 μm). Many commercial pico- and femto-second OPOs are now available. With all these achievements, it is possible, by intracavity frequency doubling the outputs (signal and idler waves), to generate blue and red light for display applications. For more detailed discussions on the SHG and OPO with ferroelectric superlattices, readers are referred to a review article by Byer (1997).

The discovery of quasicrystal in 1984 has attracted much attention on the physical effects in the quasi-periodic structure (Steinhardt and Ostlund, 1997). In the linear optics regime, quasi-periodic structure has been designed to study the effect of Anderson localization. For example, Gellermann *et al.* (1994) measured the optical transmission spectrum of quasi-periodic superlattice of SiO_2 and TiO_2 and observed a strong suppression of the transmission.

A potential application of quasi-periodic structure in nonlinear optics was first proposed by Zhu and Ming (1990). They extended the QPM technique to a quasi-periodic superlattice. In mathematics, an one-dimensional quasi-periodic lattice is just the projection of a two-dimensional periodic lattice onto a one-dimensional axis with an irrational slope, so the number of its reciprocals is more than a periodic lattice. In a quasi-periodic superlattice, the nonlinear coefficient *d(x)* is modulated quasi-periodically, can be written, using the Fourier transform approach, as

$$d(x) = \sum_{m,n} d_{m,n} \exp(iG_{m,n}x), \tag{6}$$

where the reciprocal vector $G_{m,n}=2\pi D^{-1}(m+n\tau)$, $D = \tau l_A + l_B$ is the "average structure parameter", τ = tan θ, θ is the projection angle, and $d_{m,n}$ is the

effective nonlinear coefficient of the superlattice. The $G_{m,n}$ and $d_{m,n}$ are indexed with two integers instead of one in periodic structure, showing quasi-periodic lattice more plentiful spectrum structure in wave vector space. This is very useful for the material design of QPM. Zhu *et al.* (1997) reported the first experimental result on the multi-SHG on a quasi-periodic LT superlattice. Subsequently, they (Zhu *et al.*, 1997) demonstrated that the superlattice was able to couple two QPM processes, SHG and sum-frequency generation (SFG), generating an efficient third harmonic, due to the fact two QPM conditions were simultaneously satisfied by utilizing two reciprocals, $G_{1,1}$ and $G_{2,3}$, of the superlattice. A 6 mW green light at 0.523 μm was generated from a 8-mm long LT sample with 26 mW fundamental power at 1.570 μm. The conversion efficiency of THG is 23%. This is the first example that high-order harmonics may be generated in a quadric nonlinear medium by the coupling of a number of quasi-phase-matched processes, exhibiting a possible important application of quasi-periodic structure materials in nonlinear optics. Theoretically, Zhang *et al.* (2000) studied the energy transfer among the different parametric waves in a multi-QPM interaction, and gave the conditions for optimum structure design. A periodic and three-component quasi-periodic structures were also introduced to ferroelectric superlattice, making the structure design for multi-QPM interaction more flexible.

The single-pass frequency conversion in bulk nonlinear device is limited by diffraction spreading of the focussed laser beam. The conversion efficiency can be greatly improved by confining the field to a waveguide device. The use of waveguides allows longer interaction distances at high field intensities by preventing beam spreading. Because of this, during the same period, waveguide with periodically modulated domain also attracted much attention (Webjorn *et al.*, 1989; Arbore and Fejer, 1997). By fabricating the waveguide in LT with reduced proton exchange, Yi *et al.* (1996) reached a normalized efficiency of 1500%/W, which is the highest reported for waveguide devices to date. A review of early progress in waveguide QPM materials and devices was presented by Fejer (1992).

4.3 Laser Activity

The study of doping active ions into ferroelectric superlattices has opened up a new field. Lu *et al.* first reported the growth of the Nd and Mg co-doped LN superlattice (Lu *et al.*, 1996) and the Er doped LN superlattice (Zheng *et al.*, 1998) by the Czochralski method. Strong fluorescence at various wavelengths from these doped superlattice crystals was observed, at the same time, the second harmonic of the same pump source was obtained from the same superlattice. Figure 5 displays the schematic diagram illustrating the dual-wavelength emission of the E_r doped LN superlattice. Pumped by an infrared diode laser, the superlattice with period of 5.3 μm simultaneously emitted second harmonic violet light at 404 nm by means of QPM and 547-nm green light by means of upconversion, respectively. These results show that the LN superlattices doped with laser active ions have a great potential for construction of a multi-wavelength light source by combining QPM and laser operations in the same crystal.

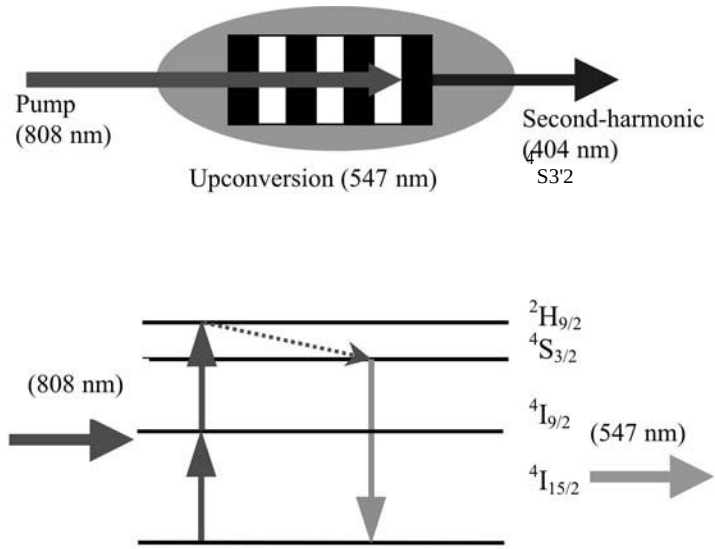

Figure 5 (a) Schematic of visible dual-wavelingth light generation, frequency upconversion green light and QPM second-harmonic violet light, in an Er:$LiNbO_3$ superlattice. (b) Energy-level diagram of Er^{3+} that depicts the energy upconversion schemes.

5 ACOUSTIC EFFECTS

It was well known that for an unpoled ferroelectric crystal, resonance at low frequencies, which are related to the geometry and dimensions of the measured sample, are absent. Only resonance at a very high frequency, which is related to the domain structure in the sample, is observed. The position of the resonant peak and its bandwidth depend on the sizes of domains and their size distribution. For a single domain ferroelectric crystal, only low frequency resonance related to the geometric sizes of the sample and its high-order harmonics can be detected, whereas high frequency resonance is absent. All resonances in a ferroelectric material, whether poled or unpoled, originate from the domains and are excited through piezoelectric effect. In a ferroelectric superlattice, piezoelectric coefficient h_{ijk}, as a third-rank tensor, is a periodic or quasi-periodic function of spatial coordinates, depending on the array of domains. The modulation of piezoelectric coefficient can result in some novel acoustic effects. It is the reason why ferroelectric superlattice sparks so much interest in ultrasonic field, and is termed

acoustic superlattice (ASL). Since 1988 Zhu *et al.* (1988; 1996) have systematically studied the excitation and propagation of elastic waves in ASL and successfully fabricated various ASL devices. Owing to piezoelectricity, the discontinuity of the piezoelectric stresses at the domain walls may be produced under the action of an external electric field. The stress must be balanced by a strain $S(u_m)$, where u_m (m = 1, 2, ...) represent the positions of the domain walls. If the external field is an alternating field, the strain can propagate as an elastic wave

$$S(u) = S(u_m)\cos(\omega t - ku), \tag{7}$$

where ω, k and t are the angle frequency, wave vector and time, respectively. Every domain wall can be viewed as a δ sound source. All domain walls in an ASL are arranged in a certain sequence forming an array (Figure 5). The elastic waves excited by this δ sound source array will interfere with each other when certain frequency condition is satisfied. Those satisfying the condition for constructive interference will appear as resonances. This is the physical basis for the ultrasonic excitation in an ASL.

As an example, considering the case of Figure 1(c), an alternating voltage is applied on the z faces of the superlattice, thus a longitudinal planar wave propagating along the z-axis will be excited inside the sample. This situation is described by the wave equation:

$$\frac{\partial^2 u_3}{\partial z^2} - \left(\frac{1}{v^2}\right)\frac{\partial^2 u_3}{\partial t^2} = \left(\frac{2h_{33}D_3}{C_{33}^D}\right)\sum_m \delta(Z - Z_m), \tag{8}$$

where u_3 represents the particle displacement along the z direction, v is the velocity of sound, h_{33} and C_{33}^D are the piezoelectric and elastic coefficients, respectively, D_3 is the component of the electric displacement along the z-axis. For an ASL with periodic domain structure, by using Green's function method to solve the elastic wave equation, the electric impedance of the ASL can be derived, and then the resonance frequency can be obtained as follows:

$$f_n = n \cdot v/(a+b), \quad n = 1, 2, 3, \ldots, \tag{9}$$

where v is the velocity of the longitudinal wave propagating along the z axis; a and b are the thickness of positive and negative domains, respectively, and $a + b$ is the period Λ of the ASL. It is obvious that the resonance frequency is determined only by the period of the ASL, i.e. $a + b$, not by the total thickness of the wafer. The thinner the laminar domains, the higher the resonance frequencies. As we know, the thickness of a resonator working at several hundred MHz is about several microns. An ordinary material with such a thickness is too thin to be fabricated by current mechanical processing methods and is too thicker to be deposited by film growth techniques. However, it is easy to grow by the Czochralski method (Zhu *et al.*, 1992) or fabricated by poling (Chen *et al.*, 1997). In practice, domain period with several microns has been achieved by using these two methods, which corresponds to resonance frequencies of hundreds MHz to several GHz (Zhu *et al.*, 1992).

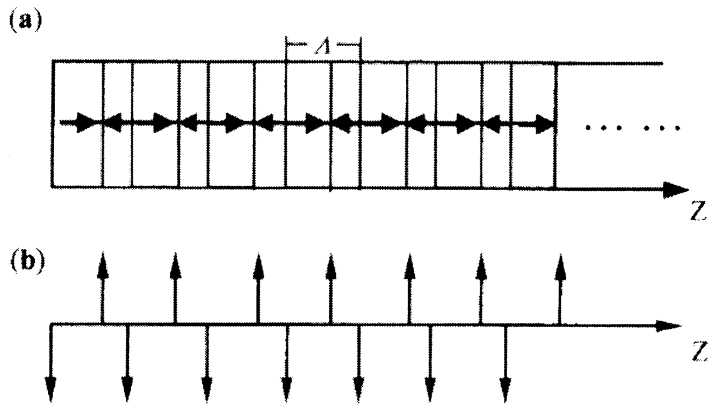

Figure 6: Schematic dagram of a ferroelectric superlattice with periodic laminar ferroelectric domain (a), and the corresponding δ - function-like sound sources (b).

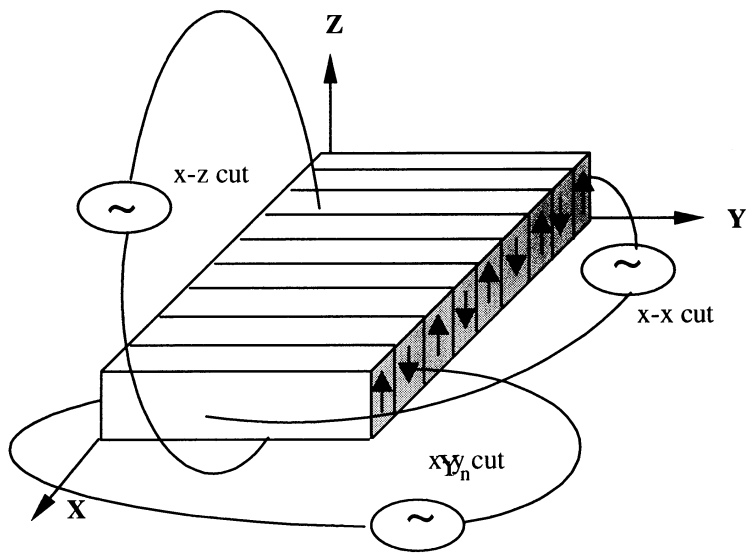

Figure 7: A schematic diagram of the ultrasonic excitation in an acoustic superlattice made of a LT crystal in which the domains are arranged periodically along the x axis, and the spontaneous polarization directions of these domains are parallel to the z axis. The excitation by the electrodes coated on the x faces (x-x cut) corresponds to the in-line scheme, while electrodes coated on the y faces (x-y cut) and the z faces (x-z cut) excite acoustic waves by the cross-field scheme. [after Chen *et al.*, 1997]

For an ASL with domain configuration like Figure 1(b), acoustic waves can be excited through two different schemes. One is an in line scheme with the acoustic propagation vector parallel to the applied electric field. The other is a cross-field scheme, which is characterized by an electric field perpendicular to the propagation vector. A schematic diagram of the two kinds of schemes is shown in Figure 7. Zhu *et al.* studied the two kinds of acoustic excitations in an ASL theoretically and Chen *et al.* (1997) experimentally confirmed their theory in the ASLs based on LT superlattices and fabricated a set of resonators operating in the range of several hundreds MHz.

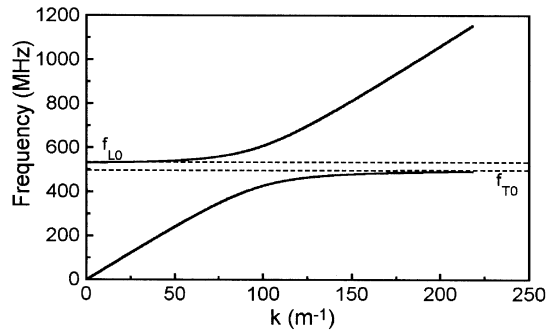

(a)

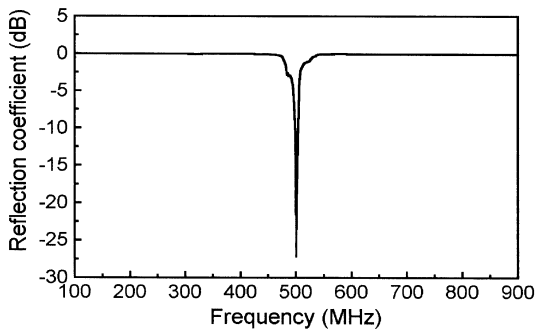

(b)

Figure 8: (a) Calculated polariton dispersion curve of an ionic-type phononic crystal with the period of 7.2 μm without consideration of damping. There is a frequency gap between f_{LO} and f_{TO} where no EM waves are permitted to propagate in the sample. (b) The measured reflection coefficient of the sample in the microwave band. The minimum of the reflection coefficient indicates that there is a strong microwave absorption peak at 502 MHz. [after Lu *et al.*, 1999]

The devices made of ASLs can be divided into two categories, resonator and transducer type, depending on their boundary conditions. For resonator, both

electrode faces of ASL are free, whereas for transducer, one face is fully matched to a transmission medium. The insertion loss of transducer is an important parameter for an acoustic device. For transducers made of homogeneous piezoelectric materials, such as a single-domain LN wafer, the static capacitance is the main part of the impedance at the resonance frequency under high-frequency operation. As a result, the insertion loss of the transducer is very high. In ASL case, the impedance of transducer may be adjusted by choosing the number of periods N and the area of the electrode face A. As a example, an insertion loss of near 0 dB at 555 MHz was achieved in a 50Ω measurement system (Zhu *et al.*, 1988).

Acoustic excitation and propagation in a quasi-periodic superlattice have been studied both theoretically and experimentally (Zhu *et al.*, 1989). The excitation spectrum in a Fibonacci superlattice is expressed by the following equation:

$$H(k) \propto \sin(kL/2) \sum (\sin X_{m,n} / X_{m,n}) \delta\{k - 2\pi(m+n\tau)/D\}, \tag{10}$$

where $X_{mn} = \pi\tau(m\tau - n)/(1+\tau^2)$ and $\tau = (1+\sqrt{5})/2$ the golden mean. The self-similarity of the Fibonacci sequence in the reciprocal space was experimentally confirmed by the acoustic excitation spectrum.

In a real crystal, various coupling exists among the motions of electrons, photons and phonons. For example, infrared absorption and polariton excitation results from the coupling between lattice vibrations and electromagnetic waves in an ionic crystal. It is expected that the same coupling may occur in artificial materials with modulated domain structures. Lu *et al.* (1999) considered a case in the ferroelectric superlattice with the "head to head" configuration (Figure 1(c)). This structure is similar to an one-dimensional diatom chain with positive and negative "ions" connected periodically. They called the superlattice an ionic-type phononic crystal (ITPC) and expected that a polariton excitation might occur in it.

In a real ionic crystal, the polariton excitation originates from the coupling of electromagnetic wave and the lattice vibration of crystal, appearing within infrared region. In an ITPC, this excitation may originate from the coupling between the superlattice vibration and electromagnetic wave. Piezoelectric effect leads to the vibration of superlattice when there is external electromagnetic field. The vibration frequency depends on the period and material constants of superlattice. So the polariton excitation in such a ferroelectric superlattice is expected to occur in the microwave region.

To verify the prediction, Lu *et al.* (1999) prepared a lithium niobate superlattice with a period of 7.2 μm and a "head to head" configuration by the growth striation method, and calculated its polariton dispersion curve. The measurement of dielectric spectrum confirmed that there was a gap between the calculated f_{T0} and f_{L0} where $\varepsilon < 0$ (Figure 8), where an incident electromagnetic wave would be strongly reflected. The measured reflection coefficient as a function of frequency showed that there was an absorption peak (~26dB) at 502 MHz. The results verified there was a polariton mode in the measured sample indeed. According to the above results, one can expect that other long-wavelength optical properties (such as Raman and Brillouin scattering *etc.*) in

a real ionic crystal also exist in such a ferroelectric superlattice. The only difference is that they occur in different frequencies, one in the infrared region (THz) and the other one in the microwave region (GHz).

6 OUTLOOK

The study of superlattice based on ferroelectric crystal has made rapid progress since 1980s. Works done in this field have a slow start due to the difficulty in material fabrication. Since it has been ascertained that a ferroelectric superlattice could be a proper candidate for quasi-phase-matched and ultrasonic excitation material, the field has been making up for the lost time. Progress in material fabrication has extended the study of ferroelectric superlattices from periodic to quasi-periodic and aperiodic (Gu *et al.*, 1999; Luo *et al.*, 2001; Zhang *et al.*, 2001; Chen *et al.*, 2001; Liu *et al.*, 2001) and then to other complicated domain patterns; and from QPM frequency conversion to the exploration of various optical and acoustic applications. For example, the generation of compressed ultrashort pulses in chirped-periodic LN and KTP superlattices were demonstrated by Alvarez *et al.*, (1999). In some recent experiments, amplitude squeezing (Serkland *et al.*, 1997), wavelength-division-multiplexing (WDM) (Chou *et al.*, 1998) have been realized. Large nonlinearity at quasi-phase mismatching conditions in ferroelectric superlattices makes it possible to use cascaded second order nonlinearity to demonstrate phase shift and optical bistability (Landry and Maldonado, 1997; Qin *et al.*, 1998). The superlattices with various modulated domains also hold great promise for use in spatial soliton systems. For example, soliton-based signal compression and shaping in QPM structures with longitudinal chirps has been proposed (Torner *et al.*, 1998). Spatial switching between different output soliton states has been predicted in QPM geometries with dislocations, tilts and wells (Clausen *et al.*, 1999). Quadratic spatial solitons by self-trapping of an optical beam were theoretically studied (Kolossovski *et al.*, 1999), and were experimentally observed in a LN superlattice (Bourliaguet *et al.*, 1999). More recently, Clausen *et al.*, (1999) analyzed nonlinear wave propagation and cascaded self-focusing in a Fibonacci superlattice and introduced the concept of quasiperiodic soliton. Such soliton has a located envelope and whose amplitude undergoes clearly detectable quasiperiodic oscillations. The result allows one to extend the concepts of self-localization and self-modulation of nonlinear waves to a broader class of spatially inhomogeneous media. On the other hand, Berger (1998) theoretically studied nonlinear frequency conversion in a two-dimensional ferroelectric superlattice (nonlinear photonic crystals). Applications as multiple-beam SHG, ring cavity SHG, or multiple wavelength frequency conversion are envisaged.

In fact, ferroelectric superlattice is one example of new materials with modulated microstructure to achieve enhanced interactions of classical waves (optical and acoustic waves) or to explore novel effects. With the development of modern technologies, other dielectric materials with various microstructure patterns are already fabricated and tailored at different spatial scales ranging from

nanometre to micron and by various methods including crystal growth, micro-processing, the assembly of small dielectric spheres, the atomic-layer-controlled-epitaxy and heteroepitaxy by molecular beam epitaxy (MBE), metal-organic chemical vapour deposition (MOCVD), chemical beam epitaxy (CBE) and so on. For example, Hu *et al.* (1996) showed laser ablation growth of LN multi-layer oriented films with periodic modulations of the z-axis direction and realized the high-frequency resonance of 10 GHz. Moreover, the acoustic-optic effect, electro-optic effect or photorefractive effect can also be used to induce superlattice structures in some ferroelectric crystals, producing significant physical phenomena when classical waves interact with them (Xu and Ming, 1993, 1993a). Recently, significant progress has been made in the growth of quantum well structures for enhanced nonlinear coefficients. Chui *et al.* (1995) have demonstrated tunable mid-IR generation in InGaAs/AlAs quantum well whose nonlinearity was measured to be 65 times more than that of the bulk GaAs. In superlattice-like photonic crystals, scientist has demonstrated how to trap or channel light (Normile, 1999). These examples show that applications of modern technologies have been leading to rapid progress on the studies of superlattice and relative devices, in which ferroelectric superlattices are included without doubt.

REFERENCES

Ahlfeldt, H., 1994, Single-domain layers formed in heat-treated $LiTaO_3$. *Applied Physics Letters*, **64**, pp. 3213-3215.

Alvarez, P. L., Reid, D. T., Faller, P., Ebrahimzadeh, M., and Sibbett, W., *et al.*, 1999, Simultaneous femtosecond-pulse compression and second-harmonic generation in a periodically poled $KTiOPO_4$. *Optics Letters*, **24**, pp. 1071-1073.

Arbore, M. A., and Fejer, M. M., 1997, Singly resonant optical parametric oscillation in periodically poled lithium niobate. *Optics Letters*, **22**, pp. 151-153.

Arbore, M. A., Galvanauskas, A., Harter, D., Chou, M. H., and Fejer, M. M., 1997, Engineerable compression of ultrashort pulses by use of second-harmonic generation in chirped-period-poled lithium niobate. *Optics Letters*, **22**, pp. 1341-1344.

Arie, A., Rosenman, G., Korenfeld, A., Skliar, A., Oron, M., Katz, M., and Eger, D., 1998, Efficient resonant frequency doubling of a cw Nd:YAG laser in bulk periodically poled $KTiOPO_4$. *Optics Letters*, **23**, pp. 28-30.

Armstrong, J. A., Bloembergen, N., Ducuing, J., and Pershan, P. S., 1962, Interactions Between Light Waves in a Nonlinear Dielectric. *Physics Review*, **127**, pp. 1918-1939.

Batchko, R. G., Shur, V. Y., Fejer, M. M., and Byer, R. L., 1999, Backswitch poling in lithium niobate for high-fidelity domain patterning and efficient blue light generation. *Applied Physics Letters*, **75**, pp. 1673-1675.

Berger, V., 1998, Nonlinear Photonic Crystals. *Physics Review Letters*, **81**, pp. 4136-4139.

Bourliaguet, B., Couderc, V., Barthelemy, G., Ross, W., Smith, P. G. R., Hanna D. C., and deAngelis, C., 1999, Observation of quadratic spatial solitons in periodically poled lithium.niobate. *Optics Letters*, **24**, pp. 1410-1412.

Burr, K. C., Tang, C. L., Arbore, M. A., and Fejer, M. M., 1997, Broadly tunable mid-infrared femtosecond optical parametric oscillator using all-solid-state pumped periodically poled lithium niobate. *Optics Letters*, **22**, pp. 1458-1460.

Byer, R. L., 1997, Quasi-phasematched nonlinear interaction and device. *Journal Nonlinear Optical Physics & Materials*, **6**, pp. 549-592.

Clausen, C. B., and Torner, L., 1999, Spatial switching of quadratic solitons in engineered quasi-phase-matched structures. *Optics Letters*, 24, pp. 7-9.

Clausen, C. B., Kivshar, Y. S., Bang, O., and Christiansen, P. L., 1999, Quasiperiodic Envelope Solitons. *Physics Review Letters*, **83**, pp. 4740-4743.

Chen, Y. B., Zhang, C., Zhu, Y. Y., Zhu, S. N., Wang, H. T., and Ming, N. B., 2001, Optical harmonic generation in a quasi-phase-matched three-component Fibonacci superlattice $LiTaO_3$. *Applied Physics Letters*, **78**, pp. 577-579.

Chen, Y. F., Zhu, S. N., Zhu, Y. Y., Ming, N. B., Jin, B. B., and Wu, R. X., 1997, High-frequency resonance in acoustic superlattice of periodically poled $LiTaO_3$. *Applied Physics Letters*, **70**, pp. 592-594.

Chiu, Y., Stancil, D. D., Schlesinger T. E., and Risk W. P., 1996, Electro-optic beam scanner in $KTiOPO_4$. *Applied Physics Letters*, **69**, pp. 3134-3136.

Chou, M. H., Parameswaran, K. R., Arbore, M. A., Hauden, J., and Fejer, M. M., 1998, in Conference on Lasers and Electro-Optics, Vol. 6 of 1998 OSA Technical Digest Series (Optical Society of America, Washington, D.C.), pp. 475.

Chui, H. C. Woods, G. L., *et al.*, 1995, Tunable mid-infrared generation by difference frequency mixing of diode laser wavelength in intersuband InGaAs/AlAs quantum wells. *Applied Physics Letters*, **66**, pp. 265-267.

Cui, Y. *et al.*, 1997, Widely tunable all-solid-state optical parametric oscillator for the visible and near infrared. *Optics Letters*, **18**, pp. 122-124.

Englander, A., Lavi, R., Katz, M., Oron, M., Eger, D., Ebiush, E. L., Rossenman, G., and Skliar, A., 1997, Highly efficient doubling of a high-repetition diode-pumped laser with bulk periodically poled KTP. *Optics Letters*, **22**, pp. 1598-1600.

Fatuzzo, E. and Merz, W. J., 1967, Ferroelectricity, North-Holland Publishing Company, Amsterdam.

Feisst, A. and Koidl, P., 1985, Current induced periodic ferroelectric domain structures in $LiNbO_3$ applied for efficient nonlinear optical frequency mixing. *Applied Physics Letters*, **47**, pp. 1125-1127.

Fejer, M. M., Magel, G. A., Jundt, D. H., and Byer, R. L., 1992, Quasi-Phase-Matched Second Harmonic Generation: Tuning and Tolerances. *Journal Quantum Electronics*, **28**, pp. 2631-2654.

Fejer, M. M, 1992, Nonlinear Optical Frequency Conversion in Periodically-poled Ferroelectric Waveguides, in Guided Wave Nonlinear Optics, ed. by D. B. Ostrowaky and R. Reinisch, Kluwer Academic Publishers, The Netherlands, pp. 133-145.

Feng, D., Ming, N. B., Hong, J. F., Yang, Y. S., Zhu, J. S., Yang, Z., and Wang, Y. N., 1980, Enhancement of second-harmonic generation in $LiNbO_3$ crystals with periodic laminar ferroelectric domains. *Applied Physics Letters*, **37**, pp. 607-609.

Gellermann, W., Kohmoto, M., Sutherland, B., and Taylor, P. C., 1994, Localization of light waves in Fibonacci dielectric multilayers. *Physics Review Letters*, **72**, pp. 633-637.

Gopalan, V., Mitchell, T. E., Furukawa, Y., and Kitamura, K., 1998, The role of nonstoichiometry in 180° domain switching of $LiNbO_3$ crystals. *Applied Physics Letters*, **72**, pp. 1981-1983.

Gu, B. Y., Dong, B. Z., Zhang, Y., and Yang, G. Z. 1999, Enhanced harmonic generation in aperiodic optical superlattices. *Applied Physics Letters*, **75**, pp. 2175-2177.

Gupta, M. C. Risk, W. P., Nutt, A. G. G., and Lau, S. D., 1993, Domain inversion in $KTiOPO_4$ using electron beam scanning. *Applied Physics Letters*, **63**, pp. 1167-1169.

Hsu, W. Y. and Gupta, M. C., 1992, Domain inversion in $LiTaO_3$ by electron beam. *Applied Physics Letters*, **60**, pp. 1-3.

Hu, W. S., Liu, Z. G., Lu, Y. Q., Zhu, S. N., and Feng, D., 1996, Pulsed-laser deposition and optical properties of completely (001) textured optical waveguiding $LiNbO_3$ films upon SiO_2/Si substrates. *Optics Letters*, **21**, pp. 946-948.

Ito, H., Takyu, C., and Inaba, H., 1991, Fabrication of periodic domain grating in $LiNbO_3$ by electron beam writing for application of nonlinear optical processes. Electronic Letters, **27**, pp. 1221-1222.

Jundt, H. D, Magel, G. A., Fejer, M. M., and Byer, R. L., 1991, Periodically poled $LiNbO_3$ for high-efficiency second-harmonic generation. *Applied Physics Letters*, **59**, pp. 2657-2659.

Keys, R. W., Loni, A., *et al.*, 1990, Fabrication of domain reversed gratings for SHG in $LiNbO_3$ by electron beam bombardment. *Electronic Letters*, **26**, pp. 188-190.

Kolossovski, K. Y., Buryak, A. V., and Sammut, R. A., 1999, Quadratic solitary waves in a counterpropagating quasi-phase-matched configuration. *Optics Letters*, **24**, pp. 835-837.

Landry, G. D. and Maldonado, T. A., 1997, Efficient nonlinear phase shifts due to cascaded second-order processes in a countpropagating quasi-phase-matched configuration. *Optics Letters*, **22**, pp. 1400-1402.

Liu, H., Zhu, Y. Y., Zhu, S. N., Zhang, C., and Ming, N. B., 2001, Aperiodic optical superlattices engineering for optical frequency conversion. *Applied Physics Letters*, **79**, pp. 728-730.

Loza-Alvarez, P., Reid, D. T., Faller, P., Ebrahimzadeh, M., and Sibbett, W., 1999, Simultaneous femtosecond-pulse compression and second-harmonic generation in aperiodically poled $KTiOPO_4$. *Optics Letters*, **24**, pp. 1071-1073.

Lu, Y. L., Cheng, X. F., Xue, C. C., and Ming, N. B., 1996, Growth of optical superlattice $LiNbO_3$ with different modulating periods and its applications in second-harmonic generation. *Applied Physics Letters*, **68**, pp. 2781-2783.

Lu, Y. L., Lu, Y. Q., Xu, C. C., and Ming, N. B., 1996, Growth of Nd^{3+}-doped $LiNbO_3$ optical superlattice crystals and its potential applications in self-frequency doubling. *Applied Physics Letters*, **68**, pp. 1467-1469.

Lu, Y. Q., Zheng, J. J., Lu, Y. L., and Ming, N. B., 1999, Frequency tuning of optical parametric generator in periodically poled optical superlattice $LiNbO_3$ by electro-optic effect. *Applied Physics Letters*, **74**, pp. 123-125.

Lu, Y. Q., Zhu, Y. Y., Chen, Y. F., Zhu, S. N., and Ming, N. B., 1999, Optical properties of an ionic-type phononic crystal. *Science*, **284**, pp. 1822-1824.

Luo, G. Z., Zhu, S. N., He, J. L., Zhu, Y. Y., Wang, H. T., Liu, Z. W., Zhang, C., and Ming, N. B., 2001, Simultaneously efficient blue and red light generations in a periodically poled $LiTaO_3$. *Applied Physics Letters*, **78**, pp. 3006-3008.

Magel, G. A., 1990, Optical second harmonic generation in Lithium Niobate Fibers. PhD thesis, Stanford University.

McGowan, C. *et al.*, 1998, Femtosecond optical parametric oscillator based on periodically poled lithium niobate. *Journal of Optical Society of America B*, **15**, pp. 694-698.

Miller, G. D., 1998, PhD thesis, Standford University.

Miller, G. D., Batchko, W. M., *et al.*, 1997, 42%-efficient single-pass CW second-harmonic generation in periodically poled lithium niobate. *Optics Letters*, **22**, pp. 1834-1836.

Ming, N. B., Hong, J. F., and Feng, D., 1982, The growth striations and ferroelectric domain structures in Czochralski-grown $LiNbO_3$ single crystals. *Journal of Material Science*, **17**, pp. 1663-1670.

Miyazawa, S., 1979, Ferroelectric domain inversion in Ti-diffused $LiNbO_3$ optical waveguide. *Journal of Applied Physics*, **50**, pp. 4599-4603.

Mizuuchi, K. and Yamamoto, K., 1994, Second-harmonic-generation in Domain-inverted Grating induced by focused ion beam. *Optical Review*, **1**, 100-102.

Mizuuchi, K., Yamamoto, K., and Kato, M., 1997, Generation of ultraviolet light by frequency doubling of a red laser diode in a first-order periodically poled bulk $LiTaO_3$. *Applied Physics Letters*, **70**, pp. 1201-1203.

Normile, D., 1999, Cages for light go from concept to reality. *Science*, **286**, pp. 1500-1502.

Peuzin, J. C., 1986, Comment on "Domain inversion effects in Ti-$LiNbO_3$ integrated optical devices". *Applied Physics Letters*, **48**, pp. 1104.

Pruneri, V., Betterworth, S. D., and Hanna, D. C., 1996, Highly efficient green-light generation by quasi-phase-matched frequency doubling of picosecond pulses from an amplified mode-locked Nd:YLF laser. *Optics Letters*, **21**, pp. 390-392.

Qin, Y. Q., Zhu, Y. Y., Zhu, S. N., and Ming, N. B., 1998, Optical bistability in periodically poled $LiNbO_3$ induced by cascaded second-order nonlinearity and electro-optic effect. *Journal of Physics: Condensed Matter*, **10**, pp. 8939-8945.

Rick, P. W. and Lau, S. D., 1996, Periodic electric field poling of $KTiOPO_4$ using chemical patterning. *Applied Physics Letters*, **69**, 3999-4001.

Robert G. B., Fejer, M. M., Byer, R. L., *et al.*, 1999, Continuous-wave quasi-phase-matched generation of 60 mW at 465 nm by single-pass frequency doubling of a

laser diode in backswitch-poled lithium niobate. *Optics Letters*, **24**, pp. 1293-1295.

Rosennman, G., Skliar, A., Eger, D., Oron, M., and Katz, M., 1998, Low temperature periodic electrical poling of flex-grown $KTiOPO_4$ and isomorphic crystals. *Applied Physics Letters*, **73**, pp. 3650-3652.

Serkland, D. K., Kumar, P., Arbore, M. A., and Fejer, M. M., 1997, Amplitude squeezing by means of quasi-phase-matched second-harmonic generation in a lithium niobate waveguide. *Optics Letters*, **22**, pp. 1497-1499.

Steinhardt, P. J. and Ostlund, S., 1997, The Physics of Quasicrystals. World Scientific, Singapore.

Tasson, M., Legal, H., Gay, J. C., Penzin, J. C., and Lissalde, F. C., 1976, Piezoelectric study of poling mechanism in lithium niobate crystal at temperature close to the Curie point. *Ferroelectrics*, **13**, pp. 479-484.

Thaniyavarn, S. Findakly, T., Booher, D., and Moen, J., 1985, Domain inversion effects in Ti-$LiNbO_3$ integrated optical devices. *Applied Physics Letters*, **46**, pp. 933-935.

Torner, L., Clausen, C. B., and Fejer, M. M., 1998, Adiabatic Shaping of Quadratic Solitions. *Optics Letters*, **23**, pp. 903-905.

Vanherzeel, H. and Bierlein, J. D., 1992, Magnitude of the nonlinear-optical coefficients of $KTiOPO_4$. *Optics Letters*, **17**, pp. 982-984.

Wang, S., Karlsson, H., and Laurell, F., 1998, In Conference on Laser and Electro-optics, Vol. 6 of 1998 *OSA Technical Digest Series* (Optical Society of America, Washington, D.C.), pp. 520.

Webjorn, J., Laurell, F., and Arvidsson, G., 1989, Blue light generated by frequency doubling of laser diode light in a lithium niobate channel waveguide. *IEEE Photonics Technique Letters*, **11**, pp. 316-318.

Wang, W.S. and Qi, M., 1986, Research on TGS single crystal growth with modulated structure. *Journal of Crystal Growth*, **79**, pp. 758-761.

Xu, B. and Ming, N. B., 1993, Optical bistability in a two-dimensional nonlinear superlattice. *Applied Physics Letters*, **71**, pp. 1003-1007.

Xu, B. and Ming, N. B. 1993, Experimental observation of bistability and instability in a two-dimensional nonlinear optical superlattice. *Physics Review Letters*, **71**, pp. 3959-3962.

Xu, H. P., Jiang, G. Z., Mao, L., Zhu, Y. Y., and Qi, M., 1992, High-frequency resonance in an acoustic superlattice of barium sodium niobate crystals. *Journal of Applied Physics*, **71**, pp. 2480-2482.

Yamada, M., Nada, N., Saitoh, M., and Watanabe. K., 1993, First-order quasi-phase-matched $LiTaO_3$ waveguide periodically poled by applying an external field for efficient blue second-harmonic generation. *Applied Physics Letters*, **62**, pp. 435-436.

Yamada, M., Saitoh, M., and Ooki, H., 1996, Electric-field induced cylindrical lens, switching and deflection devices composed of the inverted domains in $LiNbO_3$ crystal. *Applied Physics Letters*, **69**, pp. 3659-3661.

Yariv, A. and Yeh, P., 1984, Optical Waves in Crystals. John Wiley & Sons.

Yi, S. Y., Shin, S. Y., Jin, Y. S., and Son, Y. S., 1996, Second-harmonic generation in a LiTaO3 waveguide domain-inverted by proton exchange and masked heat treatment. *Applied Physics Letters*, **68**, pp. 2943-2947.

Zhang, C., Zhu, Y. Y., Yang, S. X., Qin, Y. Q., Zhu, S. N., Chen, Y. B., Liu, H., and Ming, N. B., 2000, Crucial effect of the coupling coefficients on quasi-phase- matched harmonic generation in an Optical Superlattice. *Optics Letters*, **25**, pp. 436-438.

Zheng, J. J., Lu, Y. Q., Luo, G. P. *et al.*, 1998, Visible dual-wavelength light generation in optical superlattice E_r:$LiNbO_3$ through upconversion and quasi-phase-matched frequency doubling. *Applied Physics Letters*, **72**, pp. 1808-1810.

Zhu, S. N., Zhu, Y. Y., and Ming, N. B., 1997, Quasi-Phase-Matched Third-Harmonic Generation in a Quasi-Periodic Optical Superlattice. *Science*, **278**, pp. 843-846.

Zhu, S. N., Zhu, Y. Y., Zhang, Z. Y., Shu, H., Wang, H. F., Hong, J. F. Ge, C. Z., Ming, N. B., 1995, LiTaO3 crystal periodically poled by applying an external pulsed field. *Journal Applied Physics*, **77**, pp. 5481-5483.

Zhu, S. N., Zhu, Y. Y., Qin, Y. Q., Wang, H. F., Ge, C. Z., and Ming, N. B., 1997, Experimental Realization of Second Harmonic Generation in a Fibonacci Optical Superlattice of $LiTaO_3$. *Physics Review Letters*, **78**, pp. 2752-2755.

Zhu, Y. Y., and Ming, N. B., 1990, Second-harmonic generation in a Fibonacci optical superlattice and the dispersive effect of the refractive index. *Physics Review B*, **42**, pp. 3676-3679.

Zhu, Y. Y., and Ming, N. B., 1992, Electro-optic effect and transmission spectrum in a Fibonacci optical supperlattice. *Journal of Physics: Condensed Matter*, **4**, pp. 8073-8082.

Zhu, Y. Y., and Ming, N. B., 1992, Ultrasonic excitation and propagation in an acoustic superlattice. *Journal of Applied Physics*, **72**, pp. 904-914.

Zhu, Y. Y., Ming, N. B., Jiang, W. H., and Shui, Y. A., 1988, Acoustic superlattice of LiNbO3 crystals and its applications to bulk-wave transducers for ultrasonic generation and detection up to 800 MHz. *Applied Physics Letters*, **53**, pp. 1381-1383.

Zhu, Y. Y., Ming, N. B., Jiang, W. H., 1989, Ultrasonic spectrum in Fibonacci acoustic superlattices. *Physics Review B*, **40**, pp. 8536-8538.

Zhu, Y. Y., Zhu, S. N., Hong, J. F., Ming, N. B., 1995, Domain inversion in LiNbO3 by proton exchange and quick heat treatment. *Applied Physics Letters*, **65**, pp. 558-560.

Zhu, Y. Y., Fu, J. S., Xiao, R. F., and Wong, G. K. L., 1997, Second harmonic generation in periodically domain-inverted Sr0.6Ba0.4Nb2O6 crystal plate. *Applied Physics Letters*, **70**, pp. 1793-1795.

Zhu, Y. Y. Xiao, R. F., Fu, J. S., Wong, K. L., and Ming, N. B., 1998, Third harmonic generation through coupled second-order nonlinear optical parametric processes in quasi-periodically domain-inverted $Sr_{0.6}Ba_{0.4}Nb_2O_6$ optical superlattices. *Applied Physics Letters*, **73**, pp. 432-434.